Supplemental Materials

Molecular Biology of the Cell

Lin et al.

Supplemental Information for

FAP57/WDR65 targets assembly of a subset of inner arm dyneins and connects to regulatory hubs in cilia

Jianfeng Lin[1] *, Thuc Vy Le[2] *, Katherine Augspurger[2], Douglas Tritschler[2], Raqual Bower[2], Gang Fu[1], Catherine Perrone[2], Eileen T. O'Toole[4], Kristyn VanderWaal Mills[2], Erin Dymek[3], Elizabeth Smith[3], Daniela Nicastro[1#], and Mary E. Porter[2#]

[1] Departments of Cell Biology and Biophysics, University of Texas Southwestern Medical Center, 6000 Harry Hines Blvd, Dallas, TX 75390

[2] Department of Genetics, Cell Biology and Development, University of Minnesota, Minneapolis, MN 55455

[3] Department of Biological Sciences, Class of 1978 Life Sciences Center Dartmouth College, Hanover NH 03755

[4] Department of Molecular, Cellular, and Developmental Biology, University of Colorado, Boulder, CO 80309

* authors contributed equally

[#] Corresponding authors:

Mary E. Porter, E-mail: porte001@umn.edu

Daniela Nicastro, Email: daniela.nicastro@utsouthwestern.edu

This PDF file includes:

Figures S1 to S8
Tables S1 to S5
Captions for Videos S1 to S8
References for supplemental information citations

Other supplementary materials for this manuscript include the following:

Videos S1 to S8

Supplemental Figure 1. Characterization of insertional mutations in the *IDA8* locus.

(A) The forward swimming velocities of three insertional mutant strains were measured by phase contrast light microscopy. The three strains were all significantly slower (P<0.05) than wild-type cells. **(B)** Potential defects in structure in the inner dynein arm (IDA) region were assessed by thin section electron microscopy (TEM) and computer imaging averaging (O'Toole et al., 2005). Shown here are grand averages and difference plots of the outer DMTs viewed in cross-section, with the outer arms (OA) on the bottom and the inner arms (IA) on the top. Based on contour maps, the inner arm region contains two major domains of density, an outer domain (OD) adjacent to the outer arms and an inner domain (ID) corresponding to the location of the single-headed IDAs. The three *ida8* strains showed similar structural defects in the inner domain as illustrated by the difference plots. The outer DMTs of *ida8-1* were sorted into proximal and medial/distal cross-sections and compared to WT. The defects were more prominent in the medial/distal regions of the axoneme. The number of DMT cross-sections in each average were WT (424), *ida8-1* (659), *ida8-2* (413), and *ida8-3* (183). **(C)** Genomic DNA from WT and three *ida8* strains was digested with *PvuII* and analyzed on a Southern blot probed with the pUC119 vector. **(D)** Genomic DNA from WT and three *ida8* strains was digested with *SacI* and probed with a 10 kb *NotI* fragment from the region that contains the *IDA8* gene (see Figure 1A). This fragment hybridized with 2.3 kb and 6.5 kb *SacI* restriction fragments in WT DNA. Both fragments were missing in *ida8-1*; the 2.3 kb fragment was missing in *ida8-2*, and the 6.5 kb fragment was missing in *ida8-3*. See Figure 1A for summary.

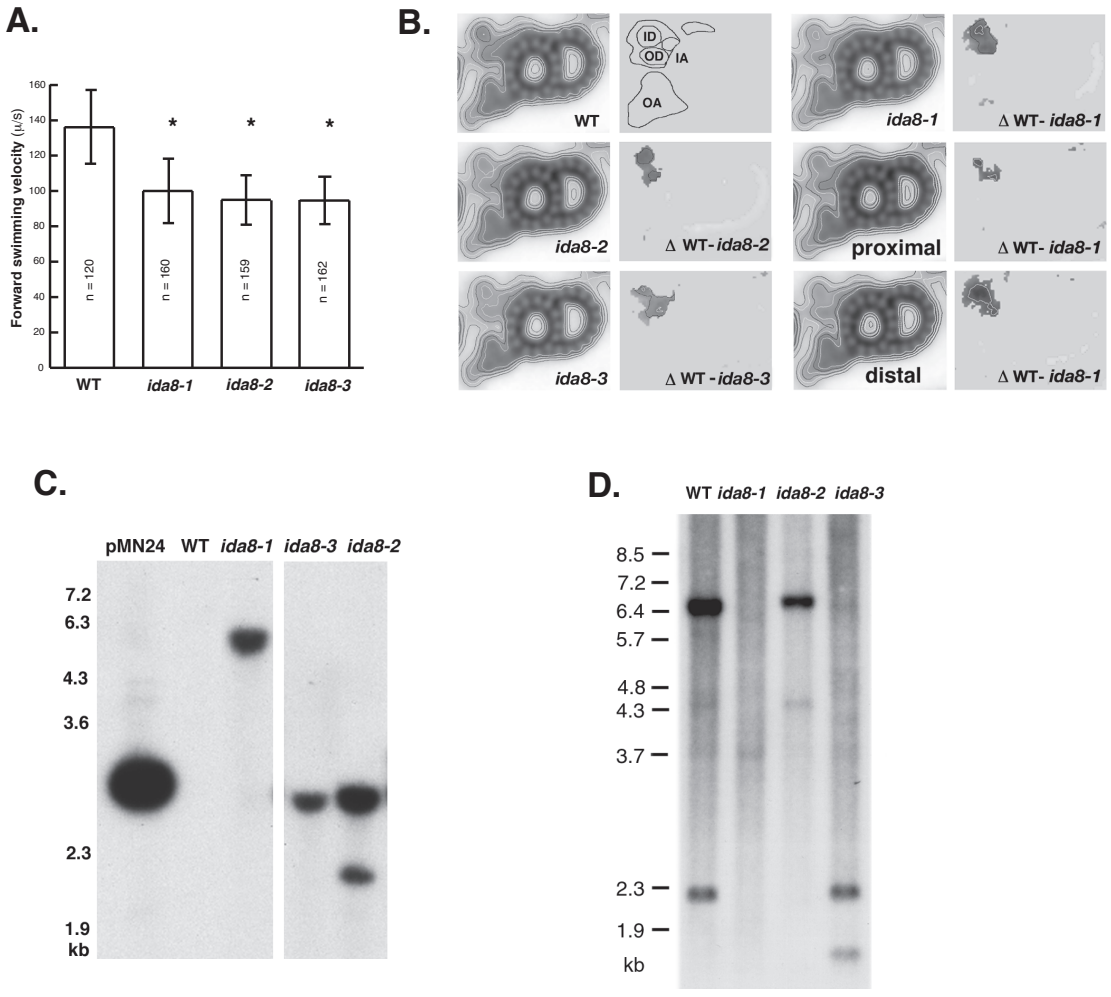

Supplemental Figure 2. Predicted amino acid sequences of FAP57 and its tagged variants

The predicted amino acid sequences of the **(A, B)** two FAP57 polypeptides generated by alternative splicing (see underlined amino acids) are shown. Also shown are epitope-tagged versions containing **(C)** a triple HA tag at the C-terminus, **(D)** a SNAP tag at the C-terminus, or **(E)** a SNAP tag at the N-terminus. The peptide sequence used to generate a FAP57 specific antibody is shown in red in **(A)**, and the sequences of the epitope tags are shown in red in (**C, D,** and **E).**

A) FAP57 variant 1 **(**Cre04.g217914.t1.1, 1316 amino acids, 146 kD)

MATSTLAPRFIFGFRADVKDNVHYAEDGSVVYPAGHNIVLYSPDTRTQRLIPGTLESEGITAICVSANKKLMAVAERSDKAMISVYDMQTL
KRRKVLVSTDAGSKEYVSLSFSGDGKTLIAQGGAPEWNLVLWVWEKSKVGSVVKTTNQQGVPMFGCAFSPGDSALVSVIGQGIFKLFR
NADAGLKAVNPVMGKRDPGLASCQCWVPDPPGSNEQRERLLLGMSDGEVLLLEGTDMKAAFSCDNGLPAVSIAAYSKGFVVGQDGG
VVTIFERDEKEFYRRARAFTIEGNACKVLNLAISPNEEHLVASLENNQAFTLLLSNQEIMKQDEMNFEVLGTPNHAGPITGLDVCVRKALI
ASCCSTDRSVRLWNWADRTCELYRTFADEIFSIAIHPTGLQVLVGFADKLRLMAVLMEDLKVVKELGIKGCRECCFSTGGQYFAAVNGT
TISIYNTYTCENVGNLRGHNGKVRSVAWSPDDSKLISAGMDGAVYEWRLKDLKRDKEHVLKGCAYASVLATPDCKLLYATGTDKKIKEF
EDSTGTGTTISKEIDTGGVNLTQLALLPNARVMFAATEAGGVRTYKYPLTGEFQEAKCHAAPVSRLRVSWDESLLVSGGEDGSVFVWE
VRDKDARAAARREQEKLEYAVEVLVTRSELDEKRSRMSELEQQVAELTMQTEYQLRLKDLHLQERVKELTDKFSGESEADRQKFEALL
AEKNEMEMEYEDKLKQAEERSQAQLQALDTQYQAKIMAEVERYQALMQEKELLAERWDEQNSLLVESHERVIAELTEDYEAKLAEEAL
KIEALQEEALKIEALQAEKAELEREFEEIKKQLEEDADREIEETKEKYEQKLQTERETSLRLKGENGIMRKKFNNLQKDIEVCNTQIKELYE
QKKELYATIASLEKDIASLKREIRERDETIGDKERRIYDLKKKNQELEKFKFVLDYKIKELKKQIEPKDLEISEMKEQIKEMDGELERYHKTN
ANLDLTISNMHLKQAGLANEVTDQRREKQDAYALMRRFQHDLQEVVGFLQEPKVLKEKVKWLYQKHCGELQSGPAEDGDVEREAARQ
REYLEKTVDSLKRKLAKDSELHRTDNLRIMQENTALIKEINELRREIKALKGAGLGAVGLGKPGSANGGAGRPGRGSPDAAAQELRREL
DMQRDLIARLREEMMMKEARIKQLEAMVVPRPISRERLPPMEGFSGAPQQPPPPSVSVASSYAPPTGMLAGGAGGPPVGLPPPSPQR
PGSAGGGGMRDSGGVVNSGAVLAGAAIAASMGPVREDSGEGYDGGAGGGQEEGFEEQEGELEGELEGELA

B) FAP57 variant 2 (Cre04.g217914.t2.1, 1306 amino acids, 145 kD)

MATSTLAPRFIFGFRADVKDNVHYAEDGSVVYPAGHNIVLYSPDTRTQRLIPGTLESEGITAICVSANKKLMAVAERSDKAMISVYDMQTL
KRRKVLVSTDAGSKEYVSLSFSGDGKTLIAQGGAPEWNLVLWVWEKSKVGSVVKTTNQQGVPMFGCAFSPGDSALVSVIGQGIFKLFR
NADAGLKAVNPVMGKRDPGLASCQCWVPDPPGSNEQRERLLLGMSDGEVLLLEGTDMKAAFSCDNGLPAVSIAAYSKGFVVGQDGG
VVTIFERDEKEFYRRARAFTIEGNACKVLNLAISPNEEHLVASLENNQAFTLLLSNQEIMKQDEMNFEVLGTPNHAGPITGLDVCVRKALI
ASCCSTDRSVRLWNWADRTCELYRTFADEIFSIAIHPTGLQVLVGFADKLRLMAVLMEDLKVVKELGIKGCRECCFSTGGQYFAAVNGT
TISIYNTYTCENVGNLRGHNGKVRSVAWSPDDSKLISAGMDGAVYEWRLKDLKRDKEHVLKGCAYASVLATPDCKLLYATGTDKKIKEF
EDSTGTGTTISKEIDTGGVNLTQLALLPNARVMFAATEAGGVRTYKYPLTGEFQEAKCHAAPVSRLRVSWDESLLVSGGEDGSVFVWE
VRDKDARAAARREQEKLEYAVEVLVTRSELDEKRSRMSELEQQVAELTMQTEYQLRLKDLHLQERVKELTDKFSGESEADRQKFEALL
AEKNEMEMEYEDKLKQAEERSQAQLQALDTQYQAKIMAEVERYQALMQEKELLAERWDEQNSLLVESHERVIAELTEDYEAKLAEEAL
KIEALQAEKAELEREFEEIKKQLEEDADREIEETKEKYEQKLQTERETSLRLKGENGIMRKKFNNLQKDIEVCNTQIKELYEQKKELYATIA
SLEKDIASLKREIRERDETIGDKERRIYDLKKKNQELEKFKFVLDYKIKELKKQIEPKDLEISEMKEQIKEMDGELERYHKTNANLDLTISNM
HLKQAGLANEVTDQRREKQDAYALMRRFQHDLQEVVGFLQEPKVLKEKVKWLYQKHCGELQSGPAEDGDVEREAARQREYLEKTVD
SLKRKLAKDSELHRTDNLRIMQENTALIKEINELRREIKALKGAGLGAVGLGKPGSANGGAGRPGRGSPDAAAQELRRELDMQRDLIAR
LREEMMMKEARIKQLEAMVVPRPISRERLPPMEGFSGAPQQPPPPSVSVASSYAPPTGMLAGGAGGPPVGLPPPSPQRPGSAGGGG
MRDSGGVVNSGAVLAGAAIAASMGPVREDSGEGYDGGAGGGQEEGFEEQEGELEGELEGELA

C) FAP57-3HA (1357 amino acids, 151 kD)

MATSTLAPRFIFGFRADVKDNVHYAEDGSVVYPAGHNIVLYSPDTRTQRLIPGTLESEGITAICVSANKKLMAVAERSDKAMISVYDMQTL
KRRKVLVSTDAGSKEYVSLSFSGDGKTLIAQGGAPEWNLVLWVWEKSKVGSVVKTTNQQGVPMFGCAFSPGDSALVSVIGQGIFKLFR
NADAGLKAVNPVMGKRDPGLASCQCWVPDPPGSNEQRERLLLGMSDGEVLLLEGTDMKAAFSCDNGLPAVSIAAYSKGFVVGQDGG
VVTIFERDEKEFYRRARAFTIEGNACKVLNLAISPNEEHLVASLENNQAFTLLLSNQEIMKQDEMNFEVLGTPNHAGPITGLDVCVRKALI
ASCCSTDRSVRLWNWADRTCELYRTFADEIFSIAIHPTGLQVLVGFADKLRLMAVLMEDLKVVKELGIKGCRECCFSTGGQYFAAVNGT
TISIYNTYTCENVGNLRGHNGKVRSVAWSPDDSKLISAGMDGAVYEWRLKDLKRDKEHVLKGCAYASVLATPDCKLLYATGTDKKIKEF
EDSTGTGTTISKEIDTGGVNLTQLALLPNARVMFAATEAGGVRTYKYPLTGEFQEAKCHAAPVSRLRVSWDESLLVSGGEDGSVFVWE
VRDKDARAAARREQEKLEYAVEVLVTRSELDEKRSRMSELEQQVAELTMQTEYQLRLKDLHLQERVKELTDKFSGESEADRQKFEALL
AEKNEMEMEYEDKLKQAEERSQAQLQALDTQYQAKIMAEVERYQALMQEKELLAERWDEQNSLLVESHERVIAELTEDYEAKLAEEAL
KIEALQEEALKIEALQAEKAELEREFEEIKKQLEEDADREIEETKEKYEQKLQTERETSLRLKGENGIMRKKFNNLQKDIEVCNTQIKELYE
QKKELYATIASLEKDIASLKREIRERDETIGDKERRIYDLKKKNQELEKFKFVLDYKIKELKKQIEPKDLEISEMKEQIKEMDGELERYHKTN
ANLDLTISNMHLKQAGLANEVTDQRREKQDAYALMRRFQHDLQEVVGFLQEPKVLKEKVKWLYQKHCGELQSGPAEDGDVEREAARQ
REYLEKTVDSLKRKLAKDSELHRTDNLRIMQENTALIKEINELRREIKALKGAGLGAVGLGKPGSANGGAGRPGRGSPDAAAQELRREL
DMQRDLIARLREEMMMKEARIKQLEAMVVPRPISRERLPPMEGFSGAPQQPPPPSVSVASSYAPPTGMLAGGAGGPPVGLPPPSPQR
PGSAGGGGMRDSGGVVNSGAVLAGAAIAASMGPVREDSGEGYDGGAGGGQEEGFEEQEGELEGELEGELAYAGGLSRYPYDYPDY
AYPYDYPDYADRSGPYPYDYAASSTR

D) FAP57-SNAP (1509 amino acids, 166.6 kD)

MATSTLAPRFIFGFRADVKDNVHYAEDGSVVYPAGHNIVLYSPDTRTQRLIPGTLESEGITAICVSANKKLMAVAERSDKAMISVYDMQTL
KRRKVLVSTDAGSKEYVSLSFSGDGKTLIAQGGAPEWNLVLWVWEKSKVGSVVKTTNQQGVPMFGCAFSPGDSALVSVIGQGIFKLFR
NADAGLKAVNPVMGKRDPGLASCQCWVPDPPGSNEQRERLLLGMSDGEVLLLEGTDMKAAFSCDNGLPAVSIAAYSKGFVVGQDGG
VVTIFERDEKEFYRRARAFTIEGNACKVLNLAISPNEEHLVASLENNQAFTLLLSNQEIMKQDEMNFEVLGTPNHAGPITGLDVCVRKALI
ASCCSTDRSVRLWNWADRTCELYRTFADEIFSIAIHPTGLQVLVGFADKLRLMAVLMEDLKVVKELGIKGCRECCFSTGGQYFAAVNGT
TISIYNTYTCENVGNLRGHNGKVRSVAWSPDDSKLISAGMDGAVYEWRLKDLKRDKEHVLKGCAYASVLATPDCKLLYATGTDKKIKEF
EDSTGTGTTISKEIDTGGVNLTQLALLPNARVMFAATEAGGVRTYKYPLTGEFQEAKCHAAPVSRLRVSWDESLLVSGGEDGSVFVWE
VRDKDARAAARREQEKLEYAVEVLVTRSELDEKRSRMSELEQQVAELTMQTEYQLRLKDLHLQERVKELTDKFSGESEADRQKFEALL
AEKNEMEMEYEDKLKQAEERSQAQLQALDTQYQAKIMAEVERYQALMQEKELLAERWDEQNSLLVESHERVIAELTEDYEAKLAEEAL
KIEALQEEALKIEALQAEKAELEREFEEIKKQLEEDADREIEETKEKYEQKLQTERETSLRLKGENGIMRKKFNNLQKDIEVCNTQIKELYE
QKKELYATIASLEKDIASLKREIRERDETIGDKERRIYDLKKKNQELEKFKFVLDYKIKELKKQIEPKDLEISEMKEQIKEMDGELERYHKTN
ANLDLTISNMHLKQAGLANEVTDQRREKQDAYALMRRFQHDLQEVVGFLQEPKVLKEKVKWLYQKHCGELQSGPAEDGDVEREAARQ
REYLEKTVDSLKRKLAKDSELHRTDNLRIMQENTALIKEINELRREIKALKGAGLGAVGLGKPGSANGGAGRPGRGSPDAAAQELRREL
DMQRDLIARLREEMMMKEARIKQLEAMVVPRPISRERLPPMEGFSGAPQQPPPPSVSVASSYAPPTGMLAGGAGGPPVGLPPPSPQR
PGSAGGGGMRDSGGVVNSGAVLAGAAIAASMGPVREDSGEGYDGGAGGGQEEGFEEQEGELEGELEGELAYAMDKDCEMKRTTLD
SPLGKLELSGCEQGLHEIKLLGKGTSAADAVEVPAPAAVLGGPEPLMQATAWLNAYFHQPEAIEEFPVPALHHPVFQQESFTRQVLWKL
LKVVKFGEVISYQQLAALAGNPAATAAVKTALSGNPVPILIPCHRVVSSSGAVGGYEGGLAVKEWLLAHEGHRLGKPGLGPAGIGAPGS

E) SNAP-FAP57 (1507 amino acids, 166.3 kD)

MDKDCEMKRTTLDSPLGKLELSGCEQGLHEIKLLGKGTSAADAVEVPAPAAVLGGPEPLMQATAWLNAYFHQPEAIEEFPVPALHHPVF
QQESFTRQVLWKLLKVVKFGEVISYQQLAALAGNPAATAAVKTALSGNPVPILIPCHRVVSSSGAVGGYEGGLAVKEWLLAHEGHRLGK
PGLGPAGIGAPGSMATSTLAPRFIFGFRADVKDNVHYAEDGSVVYPAGHNIVLYSPDTRTQRLIPGTLESEGITAICVSANKKLMAVAER
SDKAMISVYDMQTLKRRKVLVSTDAGSKEYVSLSFSGDGKTLIAQGGAPEWNLVLWVWEKSKVGSVVKTTNQQGVPMFGCAFSPGDS
ALVSVIGQGIFKLFRNADAGLKAVNPVMGKRDPGLASCQCWVPDPPGSNEQRERLLLGMSDGEVLLLEGTDMKAAFSCDNGLPAVSIA
AYSKGFVVGQDGGVVTIFERDEKEFYRRARAFTIEGNACKVLNLAISPNEEHLVASLENNQAFTLLLSNQEIMKQDEMNFEVLGTPNHA
GPITGLDVCVRKALIASCCSTDRSVRLWNWADRTCELYRTFADEIFSIAIHPTGLQVLVGFADKLRLMAVLMEDLKVVKELGIKGCRECCF
STGGQYFAAVNGTTISIYNTYTCENVGNLRGHNGKVRSVAWSPDDSKLISAGMDGAVYEWRLKDLKRDKEHVLKGCAYASVLATPDCK
LLYATGTDKKIKEFEDSTGTGTTISKEIDTGGVNLTQLALLPNARVMFAATEAGGVRTYKYPLTGEFQEAKCHAAPVSRLRVSWDESLLV
SGGEDGSVFVWEVRDKDARAAARREQEKLEYAVEVLVTRSELDEKRSRMSELEQQVAELTMQTEYQLRLKDLHLQERVKELTDKFSG
ESEADRQKFEALLAEKNEMEMEYEDKLKQAEERSQAQLQALDTQYQAKIMAEVERYQALMQEKELLAERWDEQNSLLVESHERVIAEL
TEDYEAKLAEEALKIEALQEEALKIEALQAEKAELEREFEEIKKQLEEDADREIEETKEKYEQKLQTERETSLRLKGENGIMRKKFNNLQK
DIEVCNTQIKELYEQKKELYATIASLEKDIASLKREIRERDETIGDKERRIYDLKKKNQELEKFKFVLDYKIKELKKQIEPKDLEISEMKEQIKE
MDGELERYHKTNANLDLTISNMHLKQAGLANEVTDQRREKQDAYALMRRFQHDLQEVVGFLQEPKVLKEKVKWLYQKHCGELQSGPA
EDGDVEREAARQREYLEKTVDSLKRKLAKDSELHRTDNLRIMQENTALIKEINELRREIKALKGAGLGAVGLGKPGSANGGAGRPGRGS
PDAAAQELRRELDMQRDLIARLREEMMMKEARIKQLEAMVVPRPISRERLPPMEGFSGAPQQPPPPSVSVASSYAPPTGMLAGGAGG
PPVGLPPPSPQRPGSAGGGGMRDSGGVVNSGAVLAGAAIAASMGPVREDSGEGYDGGAGGGQEEGFEEQEGELEGELEGELA

Supplemental figure 3. The distribution of the FAP57 polypeptide in different motility mutants and flagellar extracts. **(A)** A Western blot of axonemes from several mutants with defects in the ODAs, IDAs, or N-DRC was probed with antibodies against FAP57 and Rib43 as a loading control. **(B)** A Western blot of axonemes from several mutants with multiple dynein defects, central pair defects, or other uncharacterized motility defects was probed with antibodies against FAP57 and RSP16 as a loading control. **(C)** A Western blot of axonemes from the *mia1, mia2, bop2-1,* and *ida8-1* strains was probed with antibodies against FAP57, IC138, MIA1, DIC2 (IC69), and MIA2. **(D)** A Western blot of flagella (FL), a detergent-extracted, membrane plus matrix fraction (M+M), axonemes (AX), a 10 mM Mg ATP extract (ATP), a 0.6M NaCl extract (NaCl), a 0.5M NaI extract (NaI), and the final pellet of extracted outer doublets (OD) was probed with antibodies against DHC9, FAP57, the I1 subunit IC140, and the radial spoke subunit RSP16. Most of the FAP57 protein was extracted with 0.6M NaCl and the remainder with 0.6M NaI.

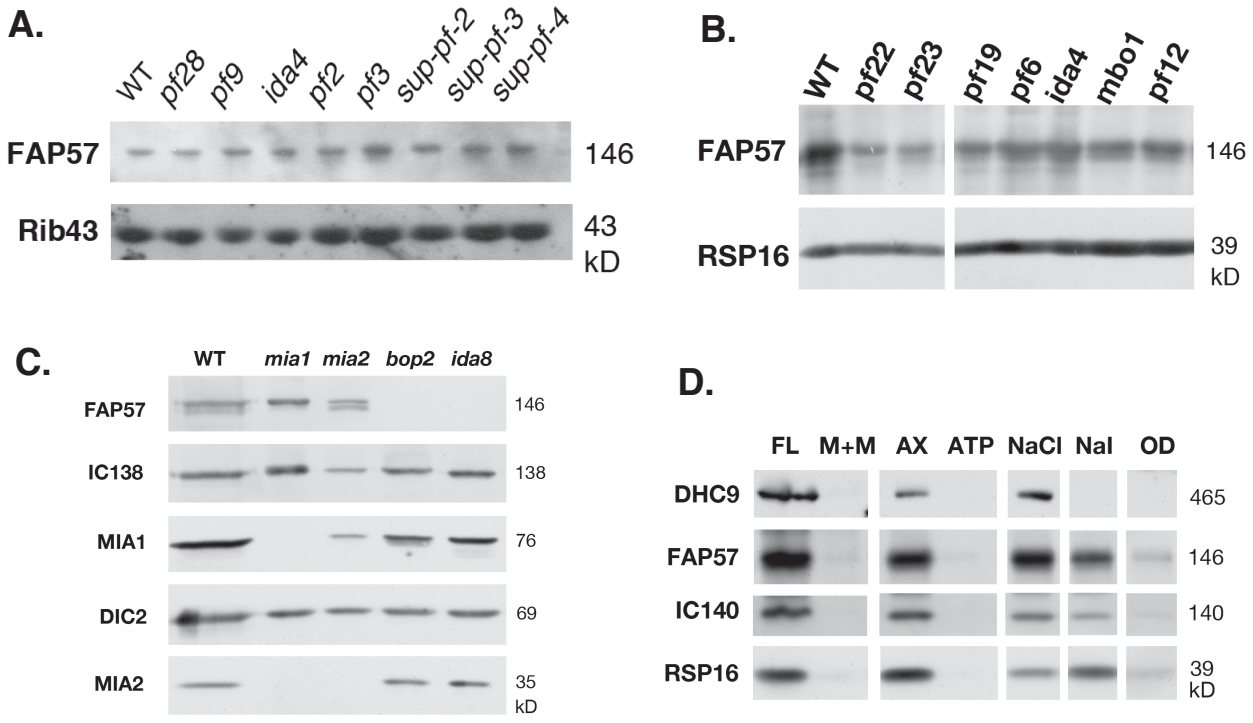

Supplemental figure 4. Phenotypic interactions between *pf10, bop2-1,* and *ida8-1.*

(A) A Western blot of axonemes from wild-type, *pf10*, and the double mutants *ida8-1; pf10* and *bop2-1; pf10* was probed with antibodies against FAP57, MBO2, and DIC2 (IC69) as a loading control. **(B)** Tracings of the flagellar waveforms observed in high speed videos of WT, *ida8-1, pf10, bop2-1, pf10* double mutants, and *FAP57-HA* rescued strains are shown here. The original videos are shown in Supplemental Videos 1-8. **(C)** Measurements of microtubule sliding velocities observed during protease-induced sliding disintegration of isolated axonemes from different strains. Values shown are mean +/- SEM. The sliding velocities of *ida8* and *bop2* were significantly slower ($P < 0.05$) than those of the WT, the FAP57 rescued strain, and *pf10*, but not significantly different from one another. The sliding velocities of *ida8; pf10* and *bop2; pf10* were also significantly slower ($P < 0.05$) than that of *pf10* alone.

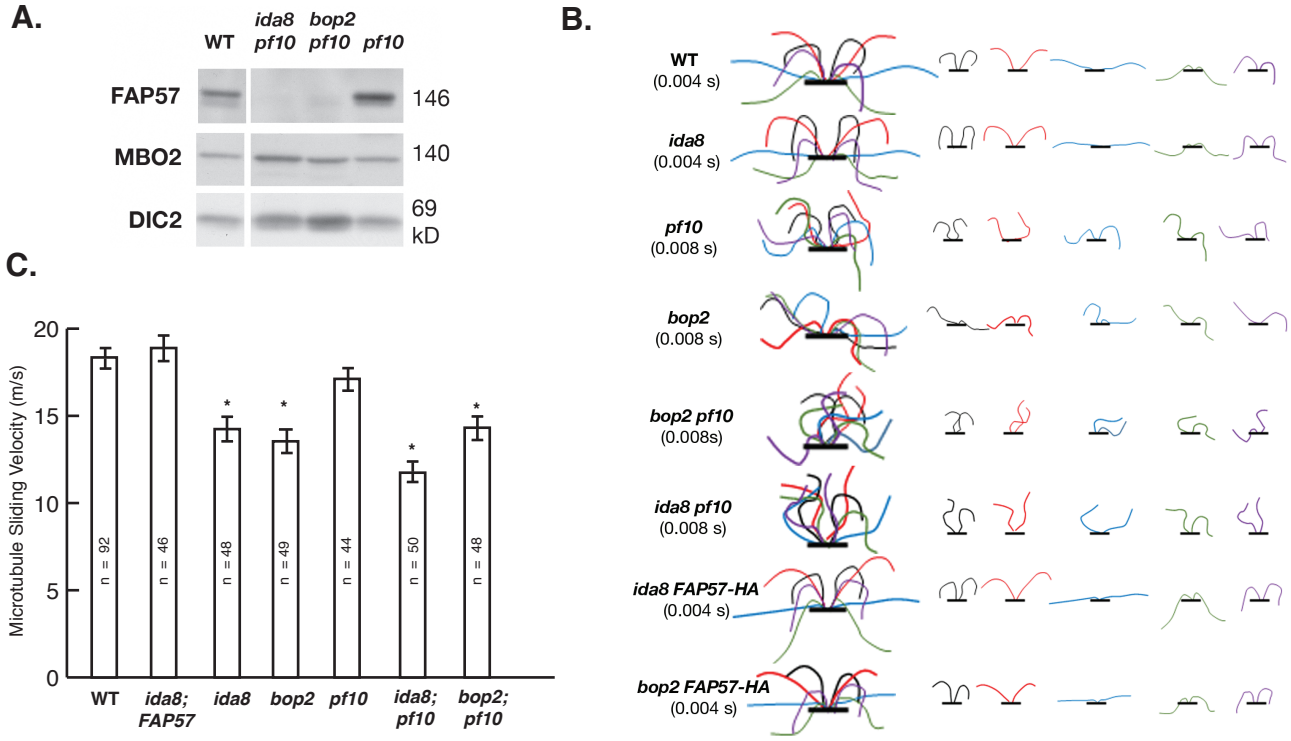

Supplemental Figure 5. Diagrams of polypeptides that are altered in *ida8* axonemes as determined by iTRAQ labeling and tandem MS/MS.

The relative sizes of the polypeptides and their predicted structural domains are drawn to scale. WD repeat domains (WD), coiled-coil domains (CC), and EF hand domains (EF).

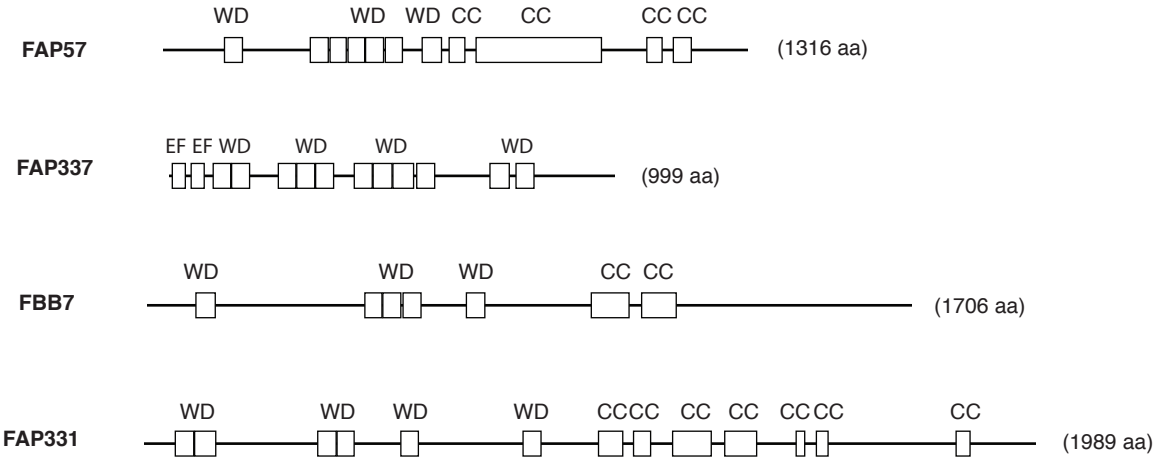

Supplemental Figure 6. Rescue of *ida8* with SNAP-tagged FAP57 constructs.

(A) Measurements of forward swimming velocities by phase contrast microscopy. FAP57 constructs containing either an N-terminal SNAP tag (*N-SNAP*) or C-terminal SNAP tag (*C-SNAP*) increased the forward swimming velocities of *ida8-1* rescued strains to near wild-type levels. **(B)** A Western blot of axonemes from WT, *ida8,* and the *C-SNAP* and *N-SNAP FAP57* rescued strains was probed with antibodies against FAP57 or the SNAP tag. Both constructs were assembled efficiently into axonemes. **(C-J**) Comparison of the averaged 96 nm repeats revealed the structural defects in *ida8* and the rescue of *ida8* with SNAP-tagged FAP57 constructs. Tomographic slices were taken from cross sections of the 96 nm repeat at the position of the I1-distal structure (C, E, G, I) or in longitudinal sections through the dyneins with the ODAs on the top and the IDAs at the bottom (D, F, H, J). The arrows indicate the I1-distal structure present in WT (C, D; red), reduced in *ida8*, (E, F; pink), and recovered in the *SNAP-N-FAP57* rescued strain (G, H; red), and the *FAP57-C-SNAP* rescued strain (I, J; red). Analysis of all *ida8* tomograms also suggested defects in the assembly of IDAs *b, g*, and *d*. However, more detailed classification analyses only confirmed the defects of I1-distal structure and IDAs *g* and *d* in *ida8,* and their recovery in rescue strains. Scale bar in (J) is 20 nm.

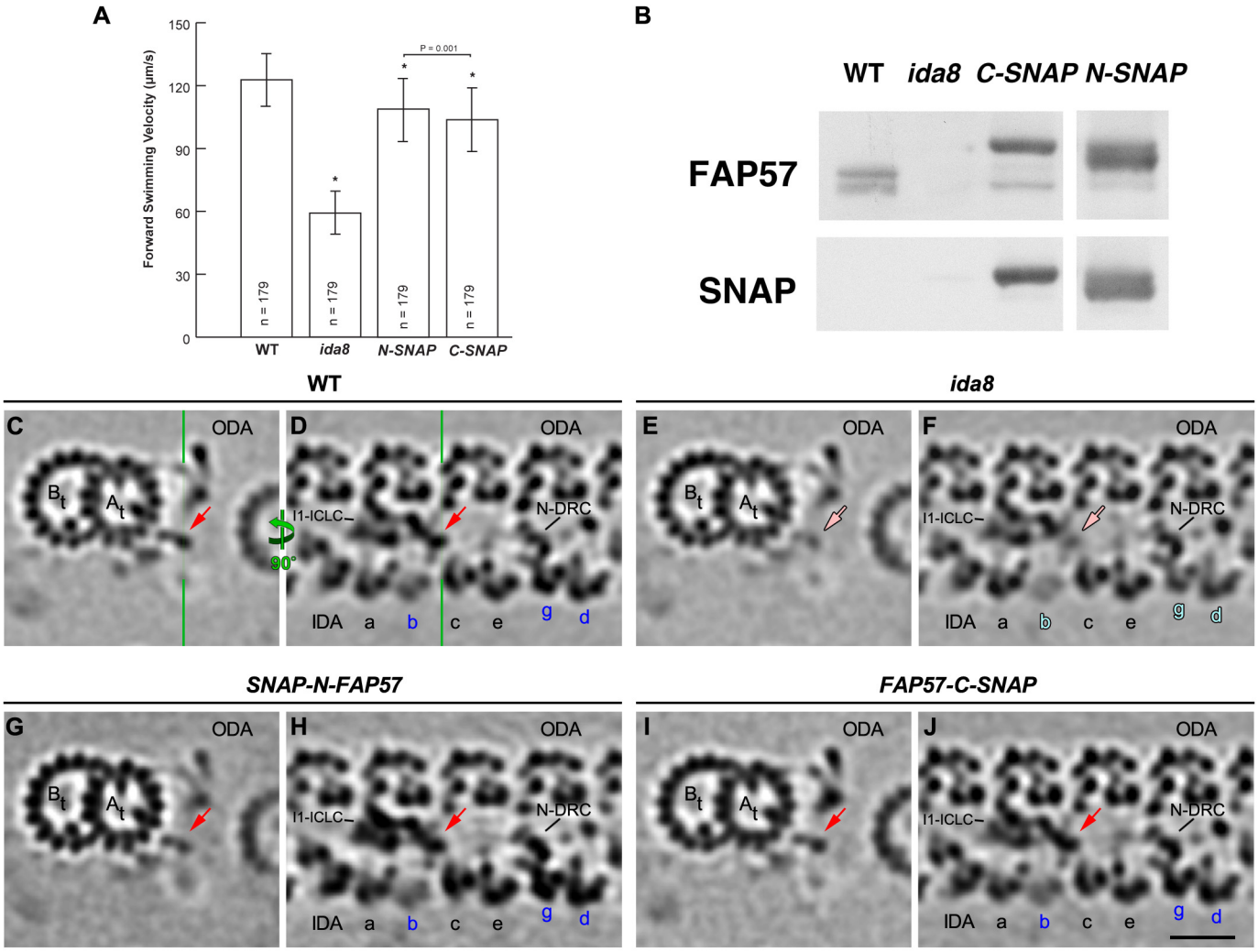

Supplemental Figure 7. Comparison of class averages of the 96 nm repeats from WT and *ida8* reveals defects in the assembly of IDAs *d* and *g* in *ida8* axonemes.

Classification analysis was performed on the 96 nm repeats from WT and *ida8* axonemes for the presence (Class 1) or absence (Class 2) of each single-headed IDA (*a, b, c, e, g, d*). Longitudinal tomographic slices of the 96 nm repeats with the four ODAs on top and the six single-headed IDAs at the bottom are shown here. The presence and absence of a given IDA structure that is indicated on the left are highlighted by blue and white arrows, respectively. The percentage of sub-tomograms included in each class average is also indicated. Note that although the percentage of tomograms that lack IDA *b* was increased in *ida8* (F, H), this increase was primarily due to the higher proportion of tomograms from the proximal region in the *ida8* dataset (see Figure 7 and Discussion). Scale bar in (X) is 20 nm.

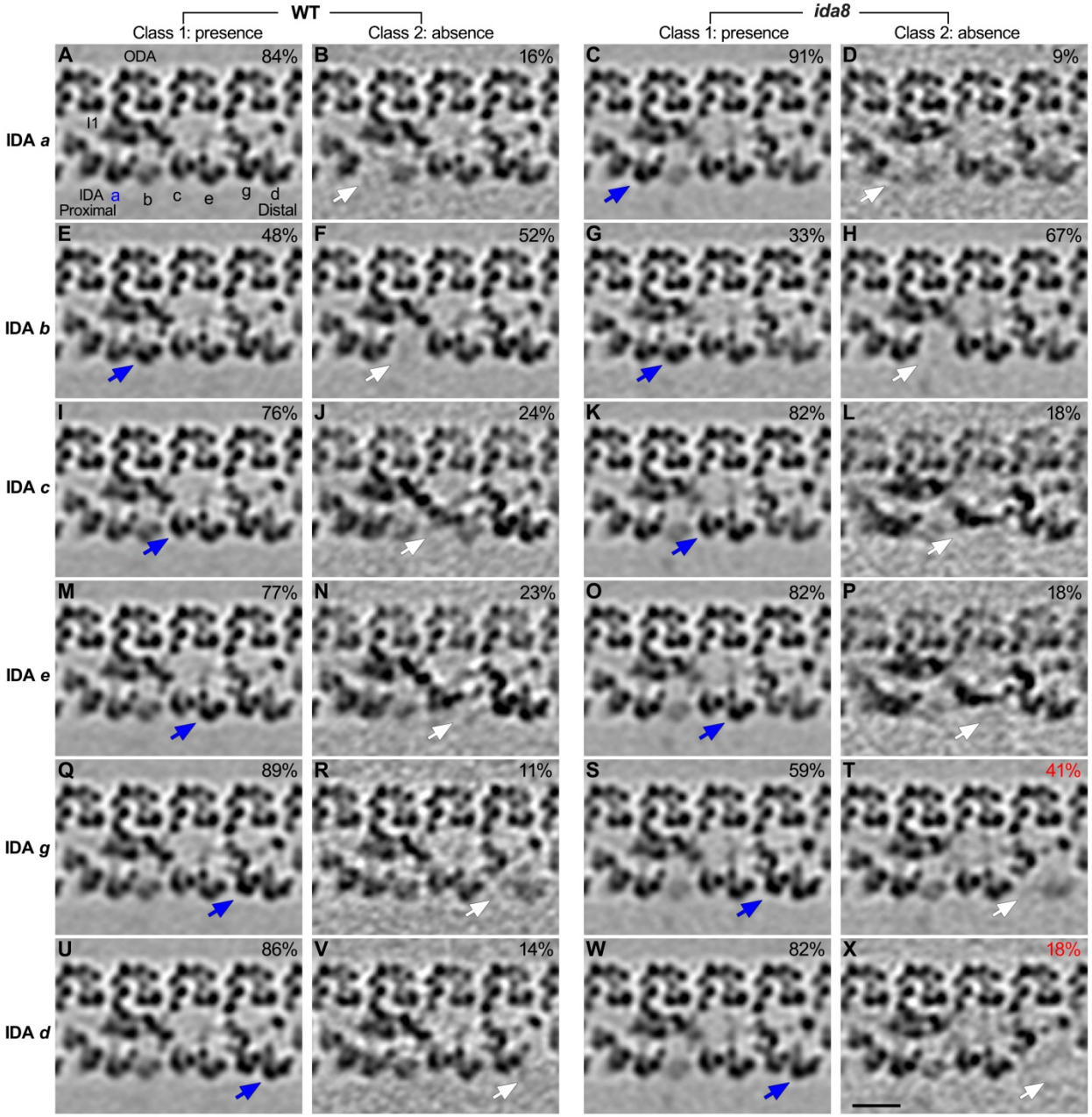

Supplemental Figure 8. DMT specific averaging reveals the asymmetric distribution of structural defects in *ida8* and their recovery in SNAP-tagged *FAP57* strains.

The 96 nm repeats on each individual DMT (1-9) were averaged for each strain (WT, *ida8, SNAP-N-FAP57* and *FAP57-C-SNAP*). Shown here are tomographic slices that were taken from longitudinal sections of the 96 nm repeats, with the ODAs on the top and the IDAs at the bottom. The red arrows indicate the normal I1-distal structure in WT and its recovery in the two rescued strains, *SNAP-N-FAP57* and *FAP57-C-SNAP*. The lighter pink arrows highlight the reduction of the I1-distal structure on DMTs 1, 5-9 in *ida8*. The dark blue arrows indicate the normal assembly of IDAs *g* and *d* in WT and the two rescued strains, *SNAP-N-FAP57* and *FAP57-C-SNAP*. The lighter blue arrows highlight the obvious reduction in the densities of IDAs *g* and *d* on DMTs 1, 5-9 in *ida8*. Scale bar is 20 nm.

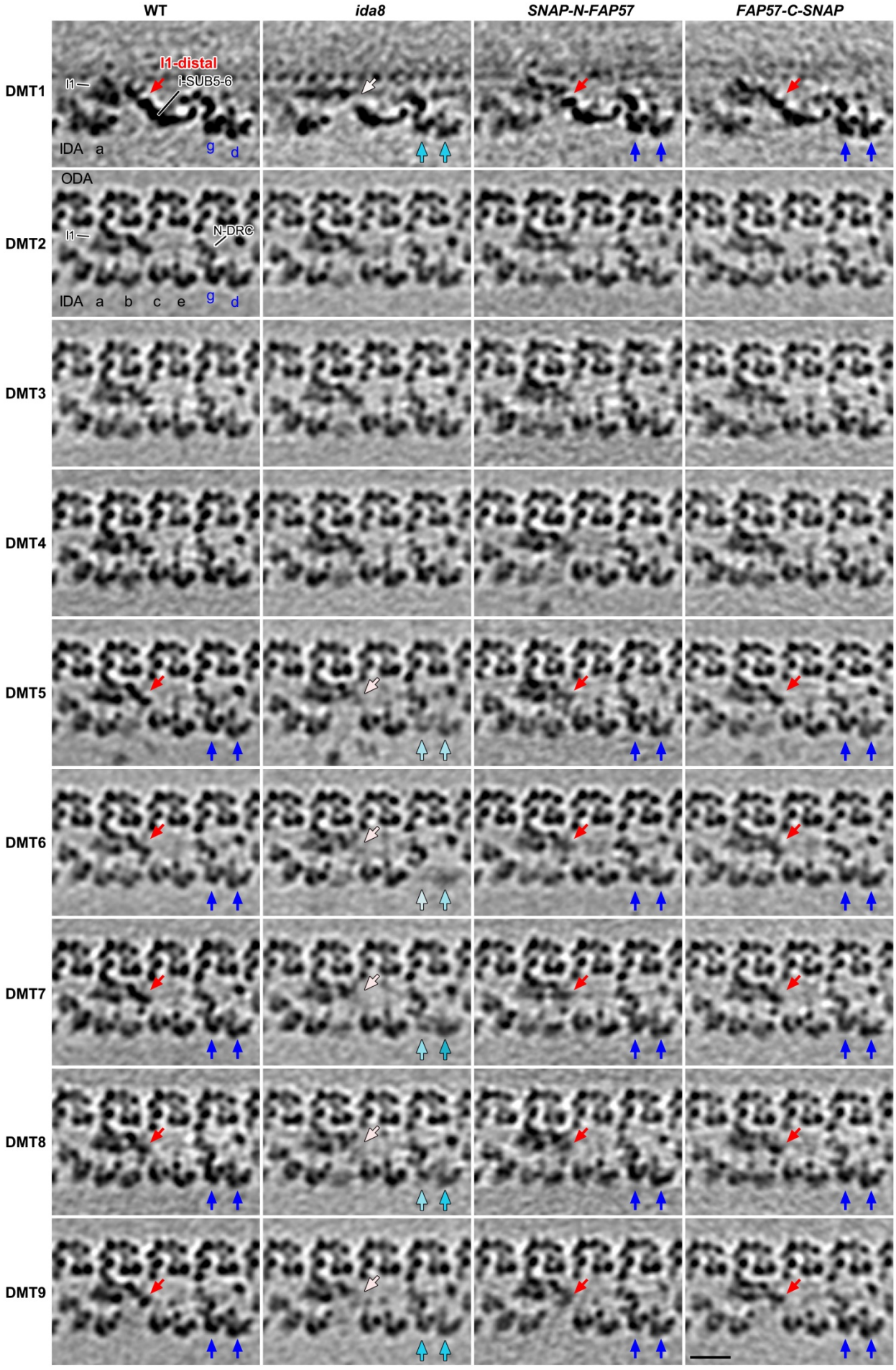
WT
ida8
SNAP-N-FAP57
FAP57-C-SNAP
DMT1
DMT2
DMT3
DMT4
DMT5
DMT6
DMT7
DMT8
DMT9
I1-distal
I1
i-SUB5-6
IDA a
g
d
ODA
N-DRC
IDA a b c e
g
d

Supplemental Table 1. Strains used in this study (available from https://www.chlamycollection.org/)

Strain name	CC number	Motility phenotype	References
Control strains			
137c, *mt-* (*nit1; nit2; agg1*)	CC-124	WT	Harris,1989
137c, *mt+* (*nit1; nit2*)	CC-125	WT	Harris,1989
L5 (*apm1-19; nit1-305; mt+*)	CC-4263	WT	Tam and Lefebvre,1993
L8 (*apm1-19; nit1-305; mt-*)	CC-4264	WT	Tam and Lefebvre,1993
arg7-8 (arg2); mt+ *arg7-8 (arg2); mt-*	CC-48 CC-1826	WT	Loppes,1969
arg7-2; mt-	CC-1820	WT	Loppes,1969
A54 e18 (*nit1-e18; ac17; sr1; mt+*)	CC-2929	WT	Harris,1989
FAP57 related			
ida8-1; mt+ (59c2)	CC-4089 CC-3928	Slow	This study
ida8-2; mt- (45g11)	CC-3929	Slow	This study
ida8-3; mt- (47d7)	CC-3930	Slow	This study
ida8-1; pf10 (4a)	CC-4090	jiggly	This study
ida8-1; pf10 (4d)	CC-4091	jiggly	This study
ida8-1; arg7-2; mt- (9c)	CC-4096	Slow	This study
ida8-1; arg7-2; mt+ (H8)	CC-4093	Slow	This study
ida8-1; FAP57 (6h9-C2)	CC-4486	WT (BAC rescue)	This study
ida8-1; FAP57 (6h9-D2)		WT (BAC rescue)	This study
ida8-1; FAP57 (6h9-E4)		WT (BAC rescue)	This study
ida8-1; FAP57 (C3)		WT (FAP57 subclone)	This study
ida8-1; FAP57 (D9)		WT (FAP57 subclone)	This study
ida8-1; FAP57-3HA1 (C8)		WT (FAP57-HA subclone)	This study
ida8-1; FAP57-3HA2 (D9)	CC-4500	WT (FAP57-HA subclone)	This study
ida8-1; FAP57-SNAP (2)	CC-5205	WT (FAP57-C-SNAP subclone)	This study
ida8-1; SNAP-FAP57 (3A)	CC-5203	WT (N-SNAP-FAP57 subclone)	This study
bop2-1; mt-	CC-4086	Slow	Dutcher et al.,1988; King et al.,1994
bop2-1; pf10 (5b)	CC-4088	jiggly	This study
bop2-1; arg7-8; mt+ (33a)	CC-4094	Slow	This study
bop2-1; FAP57; mt- (C7)	CC-4485	WT (FAP57 subclone)	This study
bop2-1; FAP57-3HA; mt- (F12)	CC-4501	WT (FAP57-HA subclone)	This study
bop2-1/ida8-1; arg7-8/arg7-2 (2A)	CC-4095	Slow (diploid)	This study
bop2-1/ida8-1; arg7-8/arg7-2 (1A)	CC-4096	Slow (diploid)	This study
bop2-1/ida8-1; arg7-8/arg7-2 (5A)	CC-4097	Slow (diploid)	This study
Dynein mutants (*Gene*)			
ida4 (DII1)	CC-2670	Slow smooth, lacks IDA *a, c, d*	Kamiya et al.,1991; Kagami & Kamiya,1992; LeDizet & Piperno,1995
ida5 (DII4/ACT1)	CC-3420	Slow smooth, lacks IDA *a, c, d, e*	Kato et al.,1993; Kato-Minoura et al.,1997
pf9-2 (DHC1)	CC-3898	Slow smooth, lacks IDA I1/*f*	Porter et al.,1992; Myster et al.,1997
pf22 (DNAAF3)	CC-1382	paralyzed, lacks ODA	Huang et al.,1979; Mitchison et al.,2012
pf23 (DYX1C1)	CC-1383	paralyzed, lacks IDA	Huang et al.,1979; Yamamoto et al.,2017
pf28 (ODA2/DHC15)	CC-1877	reduced frequency, lacks ODA	Mitchell & Rosenbaum,1985; Wilkerson et al.,1994
N-DRC mutants (*Gene*)			
pf2-4 (DRC4)	CC-4404	altered waveform DRC3-11 missing or reduced DHC2, DHC8 reduced	Huang et al.,1982; Brokaw & Kamiya,1987; Piperno et al., 1992,1994;-Rupp & Porter,2003; Heuser et al.,2009; Lin et al.,2011; Bower et al.,2013
pf3 (DRC1)	CC-1026	altered waveform DRC1-11 missing or reduced DHC8 missing other DHCs and tektin reduced	Huang et al.,1982; Brokaw & Kamiya,1987; Piperno et al., 1992,1994; Yanagisawa & Kamiya,2004; Heuser et al., 2009; Lin et al.,2011; Bower et al.,2013; 2018; Wirschell et al.,2013
sup-pf3 (DRC4)	CC-1399	reduced beat frequency DRC3-11 missing or reduced DHC8 reduced	Huang et al.,1982; Brokaw et al.,1982; Piperno et al.,1992, 1994; Heuser et al.,2009, Lin et al.,2011; Bower et al., 2013
sup-pf4 (DRC5)	CC-2366	reduced swimming velocity DRC5, 6 missing	Huang et al.,1982; Brokaw et al.,1982; Piperno et al.,1992,1994; Heuser et al., 2009; Lin et al., 2011; Bower et al., 2013
Other motility mutants (*Gene*)			
mia1-1 (FAP100)	CC-4265	phototaxis defect, altered I1 dynein	King & Dutcher, 1997; Yamamoto et al., 2013
mia2-1 (FAP73)	CC-4266	phototaxis defect, altered I1 dynein	King & Dutcher, 1997; Yamamoto et al., 2013
mbo1	CC-2679	moves backwards only symmetric waveform lacks beaks in DMT5, 6	Segal et al., 1984
pf6-2 (PF6)	CC-3926	twitchy, lacks CP projection	McVittie, 1972; Dutcher et al., 1984; Rupp et al., 2001
pf10	CC-1296	jiggling, symmetric waveform	Ramanis & Luck, 1986; Dutcher et al., 1988
pf12 (PACRG)	CC-1031	symmetric waveform reduced beaks in DMT5, 6 defective inner DMT junction	McVittie, 1972; Tam & Lefebvre, 2002; Dymek et al., 2019
pf14 (RSP3)	CC-1032	paralyzed, lacks radial spokes	Luck et al., 1977; Diener et al.,1993
pf19 (KAT1)	CC-1037	paralyzed, lacks central pair	Dutcher et al., 1984; Dymek & Smith, 2012

Supplemental Table 2. Oligonucleotide sequences used in the study

Name and purpose	Nucleotide or amino acid sequence
RT-PCR and sequencing of FAP57	
5'UTR to exon 3	5'-GGTCTTCGTTGACTTGCACAATCC-3' 5'-GCTGAATGACAGGCTCACGTATTC-3'
Exon 3 to exon 6	5'-TGGGCAGTGTGGTCAAGACG-3' 5'-TTGGAGTAGGCGGCTATGGAC-3'
Exon 6 to exon 9	5'-AGGGCAACGCCTGCAAAG-3' 5'-TGCGGTACAGCTCGCATGTC'3'
Exon 9 to exon 11	5'-CGGATCGGACATGCGAGC-3' 5'-CCTGTGGAGAAGCAGCACTCG-3'
Exon 11 to exon 13	5'-GAGTGCTGCTTCTCCACAGGC-3' 5'-CCCGTGTCGATCTCCTTGG-3'
Exon 13 to exon 15	5'-TCGACACGGGCGGCGTGAAC-3' 5'-TGCAGGTGCAGGTCCTTGAG-3'
Exon 15 to exon 19	5'-CGGAGCTGACCATGCAGACC-3' 5'-GCTGCTTCTTGATCTCCTCGAAC-3'
Exon 19 to exon 20	5'-CGGAGCTGACCATGCAGACC-3' 5'-GCCGTTCTCGCCCTTGAG-3'
Exon 20 to exon 21	5'-CAAGGGCGAGAACGGCATC-3' 5'-GGTGAGGTCCAGGTTGGC-3'
Exon 21 to exon 24	5'-GCAGATCGAGCCCAAGGACC-3' 5'-GCGTAGGAGGAGGCTACTGACAC-3'
Exon 23 to exon 24	5'-CGAGATCAAGGCACTCAAGG-3' 5'-GCGTAGGAGGAGGCTACTGACAC-3'
Exon 23 to 3'UTR	5'-GCTGGACATGCAGCGAGACC-3' 5'-GACTAGCCCCCCACCTTCG-3'
RT-PCR and sequencing of *bop2* mutation	5'-GGTCTTCGTTGACTTGCACAATCC-3' 5'-TTGGAGTAGGCGGCTATGGAC-3'
Mutagenesis and epitope tagging of FAP57	
Mutation of stop codon to create *Nde*I site	5'-GGAGGGGGAGCTGGCATATGCTGTAGCTGTGGGAGG-3' 5'-CCTCCCACAGCTACAGCATATGCCAGCTCCCCCTCC-3'
Amplification of 3-HA tag with *Nde*I sites	5'-CATATGCCGGAGGCCTGTCGCG-3' 5'-CATATGTTAGCGAGTACTGCTAGC-3'
Amplification of C-SNAP tag with *Nde*I sites	F1-5'-GGGGGAGCTGGCATATGCGATGGACAAGGACTGCGAG-3' R1-5'-CACAGCTACAGCATATGTTAGGAGCCCGGGGCGCC-3'
Synthesis of N-SNAP with *Afl*II and *Avr*II sites	CTTAAGCAGGTGGTTAGCTAGGCCAAGGAGCAGCCCTCGTTGTGCAAT TCATCGCAAACCCCTGCATGCTGCGCAAGCGGGGGCCGTCGCTACAGA GCCAAACACGAGTTCCCCCATAACGTTGACATGTTTCTTCCTTCAAGCA ATAGCTGCAACTGACCGAAGGCTTAAACAGCCAGGACCCTGAAACAGA CTTCCTTCGAGGTCCCGTTAAACGCATTGTTCACGCTGCCGCTTAGCCA CGTCAATTATAGCAAGGATTTAAAACGTAAAATTACAATTGATGCTACAT TAAGAGGGCCAAGTAGAACTCCACTCGGCACCGTGGTCTTCGTTGACTT GCACAATCCTTTAAAGACATGCAATAGCATCTAAAGTTCTTGGTATCGAC CAAATAGATAGCCGTCAGGGCTAGGGGCGCGTGGAGCAACGATGGACA AGGACTGCGAGATGAAGCGCACCACCCTGGACTCCCCGCTGGGCAAG CTGGAGCTGTCCGGCTGCGAGCAGGGCCTGCACGAGATCAAGCTGCT GGGCAAGGGCACCTCCGCCGCCGACGCCGTGGAGGTGCCGGCCCCG GCCGCCGTGCTGGGCGGCCCGGAGCCGCTGATGCAGGCCACCGCCTG GCTGAACGCCTACTTCCACCAGCCGGAGGCCATCGAGGAGTTCCCGGT GCCGGCCCTGCACCACCCGGTGTTCCAGCAGGAGTCCTTCACCCGCCA GGTGCTGTGGAAGCTGCTGAAGGTGGTGAAGTTCGGCGAGGTGATCTC CTACCAGCAGCTGGCCGCCCTGGCCGGCAACCCGGCCGCCACCGCCG CCGTGAAGACCGCCCTGTCCGGCAACCCGGTGCCGATCCTGATCCCGT GCCACCGCGTGGTGTCCTCCTCCGGCGCCGTGGGCGGCTACGAGGGC GGCCTGGCCGTGAAGGAGTGGCTGCTGGCCCACGAGGGCCACCGCCT GGGCAAGCCGGGCCTGGGCCCGGCAGGCATCGGCGCCCCGGGCTCC ATGGCGACTTCGACGCTAGCCCCTAGG

The 3-HA tag was amplified using primers with *Nde*I sites and ligated into the stop codon of a subclone. After sequence confirmation, it was ligated back into the original p59c2 plasmid to make pFAP57-3HA. To tag the C-terminus of FAP57 with SNAP, the pFAP57-3HA plasmid was digested with *Nde*I to release the HA tag and the SNAP tag was amplified with the primers listed above for direct cloning into the *Nde*I site using the In-Fusion cloning kit (Thermo Scientific).

Supplemental Table 3. Antibodies used in this study

Antigen	Host	Dilution (WB)	Reference or source
DRC1	Rabbit	1:1000-1:10000	Wirschell et al., 2013
Gas8 fusion (DRC4)	Rabbit	1:1000-1:10000	Bower et al., 2013
CCDC39/FAP59	Rabbit	1:1000	Sigma #HPA035364
FAP57	Rabbit	1:1000-5000	This study
Rib43	Rabbit	1:10000-1:20000	Norrander et al., 2000
Rib72	Rabbit	1:10000-1:20000	Ikeda et al., 2003
tektin	Rabbit	1:20000	Yanagisawa & Kamiya, 2004
DHC5	Rabbit	1:1000	Yagi et al., 2009
DHC9	Rabbit	1:5000	Yagi et al., 2009
IC140	Rabbit	1:10000	Yang & Sale, 1998
IC2 (IC69)	Mouse	1:10000-1:20000	Sigma #D6168
IC138	Rabbit	1:10000	Hendrickson et al., 2004
MIA1	Rabbit	1:1000	Yamamoto et al., 2013
MIA2	Rabbit	1:1000	Yamamoto et al., 2013
MBO2	Rabbit	1:1000	Tam and Lefebvre, 2002
RSP16	Rabbit	1:10000-1:20000	Yang et al., 2005
HA (3F10)	Rat	1:500-1000	Roche #1867423
GFP	Mouse	1:5000	Covance #MMS-118P
SNAP	Rabbit	1:1000	New England Biolabs #P9310S

Supplemental Table 4. Polypeptides co-eluting with FAP57 in FPLC peak *g*

Protein	*Chlamydomonas* ID	Peptides (N)	Length (aa) and MW (kD)	Predicted domains	Best hit in *H. sapiens*[a]
FAP44	Cre09.g386736	44	2141 (222)	WD, CC	WDR52
FAP43	Cre16.g691440	34	1950 (199)	WD, CC	WDR96
FAP57	Cre04.g217914	24	1316 (146)	WD, CC	WDR65
DHC7	Cre14.g627576	32	4191 (468)	AAA, CC	DNAH6
FAP244	Cre08.g374700	7	2630 (267)	WD, CC	N.D.
IFT88	Cre07.g335750	7	782 (86)	TPR	IFT88
1α DHC	Cre12.g484250	5	4626 (523)	AAA, CC	DNAH10
Actin	Cre13.g603700	5	377 (42)		Actin
FAP159	Cre01.g022750	3	2577 (252)	LRR	N.D.
FAP75	Cre06.g249900	3	1264 (125)	AAA	AK7
IC97 (DII6)	Cre14.g631200	3	760 (82)	CC	CASC1

[a]Best hits were identified by blasting the predicted amino acid sequences in version 5.6 of the *Chlamydomonas* genome project (https://phytozome-next.jgi.doe.gov/info/Creinhardtii_v5_6) against the NCBI database.

Table S5. *Chlamydomonas* strains used for cryo ET analyses

Strain	Number of tomograms	Averaged repeats	Resolution 0.5 FSC (nm)
WT-I[a)] (F30/CCD data)	25	3736	3.4
WT-II[b)] (Krios/K2/VPP data; higher resolution)	80	11225	1.8
ida8	33	4227	3.8
SNAP-N-FAP57 control	12	1500	3.6
SNAP-N-FAP57+Au	18	2207	3.6
FAP57-C-SNAP control	10	1500	4.1
FAP57-C-SNAP+Au	16	2498	3.7

a) The WT-I reference dataset is a composite of tomograms from WT (CC-125), *ida6::IDA6-GFP* (CC-4495), *DRC3-SNAP* (CC-5243), and *SNAP-DRC3* (CC-5244) axonemes. Some of these tomograms were previously used to analyze other axonemal complexes (Song et al., 2015; Bower et al., 2018). The *ida6::IDA6-GFP* strain was generated by rescuing *ida6* with a GFP-tagged WT *IDA6* gene (Bower et al., 2018). The *DRC3-SNAP* and *SNAP-DRC3* strains were generated by rescuing *drc3* with the WT *DRC3* gene tagged with SNAP at either its N-terminal or C-terminal end (Awata et al., 2015; Song et al., 2015). All of these axonemes are structurally and phenotypically indistinguishable from WT.

b) The WT-II reference dataset is a composite of tomograms from WT (CC-4533) and several central pair mutants (*fap76-1*, *fap81*, *fap92*, *fap216,* and *fap76-1; fap81*) obtained from the *Chlamydomonas* CLiP library (CLiP ID numbers: LMJ.RY0402.089534, LMJ.RY0402.092632, LMJ.RY0402.204383, and LMJ.RY0402.218389, respectively). Some of these tomograms were previously used to analyze other axonemal complexes (Fu et al. 2019). The 96nm axoneme repeats in the central pair mutants are structurally indistinguishable from WT.

Captions for Videos S1 to S8

Supplemental Video S1. Video of a wild-type cell swimming forward with an asymmetric waveform.

Supplemental Video S2. Video of an *ida8-1* cell swimming forward with an asymmetric waveform.

Supplemental Video S3. Video of a *bop2-1* cell swimming forward with an asymmetric waveform.

Supplemental Video S4. Video of an *ida8-1; Fap57-HA* rescued cell swimming forward with an asymmetric waveform.

Supplemental Video S5. Video of a *bop2-1, FAP57-HA* rescued cell swimming forward with an asymmetric waveform.

Supplemental Video S6. Video of a *pf10* cell swimming with an abnormal waveform.

Supplemental Video S7. Video of an *ida8-1; pf10* cell swimming with a variable waveform.

Supplemental Video S8. Video of a *bop2-1; pf10* cell swimming with a variable waveform.

Supplemental References

Awata, J., K. Song, J. Lin, S.M. King, M.J. Sanderson, D. Nicastro, and G.B. Witman. 2015. DRC3 connects the N-DRC to dynein g to regulate flagellar waveform. *Mol. Biol. Cell.* 26:2788-2800.

Bower, R., D. Tritschler, K.V. Mills, T. Heuser, D. Nicastro, and M.E. Porter. 2018. DRC2/CCDC65 is a central hub for assembly of the nexin-dynein regulatory complex and other regulators of ciliary and flagellar motility. *Mol. Biol. Cell.* 29:137-153.

Bower, R., D. Tritschler, K. Vanderwaal, C.A. Perrone, J. Mueller, L. Fox, W.S. Sale, and M.E. Porter. 2013. The N-DRC forms a conserved biochemical complex that maintains outer doublet alignment and limits microtubule sliding in motile axonemes. *Mol. Biol. Cell.* 24:1134-1152.

Brokaw, C.J., and R. Kamiya. 1987. Bending patterns of *Chlamydomonas* flagella: IV. Mutants with defects in inner and outer dynein arms indicate differences in dynein arm function. *Cell Motil. Cytoskeleton*. 8:68-75.

Brokaw, C.J., D.J. Luck, and B. Huang. 1982. Analysis of the movement of *Chlamydomonas* flagella: the function of the radial-spoke system is revealed by comparison of wild-type and mutant flagella. *J. Cell Biol*. 92:722-732.

Dutcher, S.K., W. Gibbons, and W.B. Inwood. 1988. A genetic analysis of suppressors of the *PF10* mutation in *Chlamydomonas reinhardtii*. *Genetics*. 120:965-976.

Dutcher, S.K., B. Huang, and D.J.L. Luck. 1984. Genetic dissection of the central pair microtubules of the flagella of *Chlamydomonas reinhardtii. J. Cell Biol.* 98:229-236.

Dymek, E.E., J. Lin, G. Fu, M. Porter, D. Nicastro, and E.F. Smith. 2019. PACRG and FAP20 form the inner junction of axonemal doublet microtubules and regulate ciliary motility. *Mol. Biol. Cell.* mbcE19-01-0063.

Fu, G., L. Zhao, E. Dymek, Y. Hou, K. Song, N. Phan, Z. Shang, E.F. Smith, G.B. Witman, and D. Nicastro. 2019. Structural organization of the C1a-e-c supercomplex within the ciliary central apparatus. *J. Cell Biol.* Under review.

Gardner, L.C., E. O'Toole, C.A. Perrone, T. Giddings, and M.E. Porter. 1994. Components of a "dynein regulatory complex" are located at the junction between the radial spokes and the dynein arms in Chlamydomonas flagella. *J. Cell Biol.* 127:1311-1325.

Harris, E. 1989. The *Chlamydomonas* Sourcebook. Academic Press, San Diego, CA. 780 pp.

Hendrickson, T.W., C.A. Perrone, P. Griffin, K. Wuichet, J. Mueller, P. Yang, M.E. Porter, and W.S. Sale. 2004. IC138 is a WD-repeat dynein intermediate chain required for light chain assembly and regulation of flagellar bending. *Mol. Biol. Cell.* 15:5431-5442.

Heuser, T., M. Raytchev, J. Krell, M.E. Porter, and D. Nicastro. 2009. The dynein regulatory complex is the nexin link and a major regulatory node in cilia and flagella. *J. Cell Biol.* 187:921-933.

Huang, B., G. Piperno, and D.J. Luck. 1979. Paralyzed flagella mutants of *Chlamydomonas reinhardtii*. Defective for axonemal doublet microtubule arms. *J. Biol. Chem*. 254:3091-3099.

Huang, B., Z. Ramanis, and D.J. Luck. 1982. Suppressor mutations in *Chlamydomonas* reveal a regulatory mechanism for flagellar function. *Cell*. 28:115-124.

Ikeda, K., J.A. Brown, T. Yagi, J.M. Norrander, M. Hirono, E. Eccleston, R. Kamiya, and R.W. Linck. 2003. Rib72, a conserved protein associated with the ribbon compartment of flagellar A-microtubules and potentially involved in the linkage between outer doublet microtubules. *J. Biol. Chem*. 278:7725-7734.

Kagami, O., and R. Kamiya. 1992. Translocation and rotation of microtubules caused by multiple species of *Chlamydomonas* inner-arm dynein. *J. Cell Sci.* 103:653-664.

Kamiya, R., E. Kurimoto, and E. Muto. 1991. Two types of *Chlamydomonas* flagellar mutants missing different components of inner-arm dynein. *J. Cell Biol.* 112:441-447.

Kato, T., O. Kagami, T. Yagi, and R. Kamiya. 1993. Isolation of two species of *Chlamydomonas reinhardtii* flagellar mutants, *ida5* and *ida6*, that lack a newly identified heavy chain of the inner dynein arm. *Cell Struct. Funct.* 18:371-377.

Kato-Minoura, T., M. Hirono, and R. Kamiya. 1997. *Chlamydomonas* inner-arm dynein mutant, *ida5*, has a mutation in an actin-encoding gene. *J. Cell Biol.* 137:649-656.

King, S.J., and S.K. Dutcher. 1997. Phosphoregulation of an inner dynein arm complex in *Chlamydomonas reinhardtii* is altered in phototactic mutant strains. *J. Cell Biol.* 136:177-191.

King, S.J., W.B. Inwood, E.T. O'Toole, J. Power, and S.K. Dutcher. 1994. The *bop2-1* mutation reveals radial asymmetry in the inner dynein arm region of *Chlamydomonas reinhardtii*. *J. Cell Biol.* 126:1255-1266.

Kollmar, M. 2016. Fine-Tuning Motile Cilia and Flagella: Evolution of the Dynein Motor Proteins from Plants to Humans at High Resolution. *Mol. Biol. Evol*. 33:3249-3267.

Lin, J., D. Tritschler, K. Song, C.F. Barber, J.S. Cobb, M.E. Porter, and D. Nicastro. 2011. Building blocks of the nexin-dynein regulatory complex in *Chlamydomonas* flagella. *J. Biol. Chem*. 286:29175-29191.

Loppes, R. 1969. A new class of arginine-requiring mutants in *Chlamydomonas reinhardii*. *Mol. & Gen. Genet.* 104:172-177.

Luck, D.J.L., G. Piperno, Z. Ramanis, and B. Huang. 1977. Flagellar mutants of *Chlamydomonas*: Studies of radial spoke-defective strains by dikaryon and revertant analysis. *Proc. Natl. Acad. Sci. U.S.A*. 74:3456-3460.

Mastronarde, D.N., E.T. O'Toole, K.L. McDonald, J.R. McIntosh, and M.E. Porter. 1992. Arrangement of inner dynein arms in wild-type and mutant flagella of *Chlamydomonas*. *J. Cell Biol.* 118:1145-1162.

McVittie, A. 1972. Flagellum mutants of *Chlamydomonas reinhardtii*. *J. Gen. Microbiol*. 71:525-540.

Mitchell, D.R., and J.L. Rosenbaum. 1985. A motile *Chlamydomonas* flagellar mutant that lacks outer dynein arms. *J. Cell Biol.* 100:1228-1234.

Norrander, J.M., A.M. deCathelineau, J.A. Brown, M.E. Porter, and R.W. Linck. 2000. The Rib43a protein is associated with forming the specialized protofilament ribbons of flagellar microtubules in *Chlamydomonas*. *Mol. Biol. Cell.* 11:201-215.

O'Toole, E., D. Mastronarde, J.R. McIntosh, and M.E. Porter. 1995. Computer-assisted image analysis of flagellar mutants. *Meth. Cell Biol.* 47:183-191.

Piperno, G. 1995. Regulation of dynein activity within *Chlamydomonas* flagella. *Cell Motil. Cytoskeleton*. 32:103-105.

Piperno, G., K. Mead, M. LeDizet, and A. Moscatelli. 1994. Mutations in the "dynein regulatory complex" alter the ATP-insensitive binding sites for inner arm dyneins in *Chlamydomonas* axonemes. *J. Cell Biol.* 125:1109-1117.

Piperno, G., K. Mead, and W. Shestak. 1992. The inner dynein arms I2 interact with a "dynein regulatory complex" in *Chlamydomonas* flagella. *J. Cell Biol.* 118:1455-1463.

Porter, M.E., J. Power, and S.K. Dutcher. 1992. Extragenic suppressors of paralyzed flagellar mutations in *Chlamydomonas reinhardtii* identify loci that alter the inner dynein arms. *J. Cell Biol.* 118:1163-1176.

Ramanis, Z., and D.J. Luck. 1986. Loci affecting flagellar assembly and function map to an unusual linkage group in *Chlamydomonas reinhardtii*. *Proc. Natl. Acad. Sci. U. S. A*. 83:423-426.

Rupp, G., E. O'Toole, and M.E. Porter. 2001. The *Chlamydomonas PF6* locus encodes a large alanine/proline-rich polypeptide that is required for assembly of a central pair projection and regulates flagellar motility. *Mol. Biol. Cell.* 12:739-751.

Rupp, G., and M.E. Porter. 2003. A subunit of the dynein regulatory complex in *Chlamydomonas* is a homologue of a growth arrest-specific gene product. *J. Cell Biol.* 162:47-57.

Segal, R.A., B. Huang, Z. Ramanis, and D.J.L. Luck. 1984. Mutant strains of *Chlamydomonas reinhardtii* that move backwards only. *J. Cell Biol.* 98:2026-2034.

Song, K., J. Awata, D. Tritschler, R. Bower, G.B. Witman, M.E. Porter, and D. Nicastro. 2015. In Situ Localization of N and C Termini of Subunits of the Flagellar Nexin-Dynein Regulatory Complex (N-DRC) Using SNAP Tag and Cryo-electron Tomography. *J. Biol. Chem*. 290:5341-5353.

Tam, L.W., and P.A. Lefebvre. 1993. Cloning of flagellar genes in *Chlamydomonas reinhardtii* by DNA insertional mutagenesis. *Genetics*. 135:375-384.

Tam, L.W., and P.A. Lefebvre. 2002. The *Chlamydomonas MBO2* locus encodes a conserved coiled-coil protein important for flagellar waveform conversion. *Cell Motil. Cytoskeleton*. 51:197-212.

Warr, J.R., A. McVittie, J.T. Randall, and J.M. Hopkins. 1966. Genetic control of flagellar structure in *Chlamydomonas reinhardtii*. *Genet. Res. Camb.* 7:335-351.

Wirschell, M., H. Olbrich, C. Werner, D. Tritschler, R. Bower, W.S. Sale, N.T. Loges, P. Pennekamp, S. Lindberg, U. Stenram, B. Carlen, E. Horak, G. Kohler, P. Nurnberg, G. Nurnberg, M.E. Porter, and H. Omran. 2013. The nexin-dynein regulatory complex subunit DRC1 is essential for motile cilia function in algae and humans. *Nat Genet*. 45(3):262-8

Yagi, T., K. Uematsu, Z. Liu, and R. Kamiya. 2009. Identification of dyneins that localize exclusively to the proximal portion of *Chlamydomonas* flagella. *J. Cell Sci*. 122:1306-1314.

Yamamoto, R., K. Song, H.A. Yanagisawa, L. Fox, T. Yagi, M. Wirschell, M. Hirono, R. Kamiya, D. Nicastro, and W.S. Sale. 2013. The MIA complex is a conserved and novel dynein regulator essential for normal ciliary motility. *J. Cell Biol*. 201:263-278.

Yanagisawa, H.A., and R. Kamiya. 2004. A tektin homologue is decreased in *Chlamydomonas* mutants lacking an axonemal inner-arm dynein. *Mol. Biol. Cell.* 15:2105-2115.

Yang, C., M.M. Compton, and P. Yang. 2005. Dimeric novel HSP40 is incorporated into the radial spoke complex during

the assembly process in flagella. *Mol. Biol. Cell.* 16:637-648.
Yang, P., and W.S. Sale. 1998. The Mr 140,000 intermediate chain of *Chlamydomonas* flagellar inner arm dynein is a WD-repeat protein implicated in dynein arm anchoring. *Mol. Biol. Cell.* 9:3335-3349.